Effects of Laser Surface Melting on the Pitting Resistance of Sensitized Nitrogen-Bearing Type 316L Stainless Steel

U. Kamachi Mudali, M.G. Pujar, and R.K. Dayal

(Submitted 15 July 1997; in revised form 19 December 1997)

Laser surface melting of sensitized nitrogen-bearing type 316L austenitic stainless steel was carried out using a pulsed ruby laser. The sensitization heat treatment was carried out at 923 K for 50, 200, 1000, and 2500 h, and the sensitized microstructure was classified according to ASTM A 262 practice A. The degree of sensitization was assessed by the electrochemical potentiokinetic reactivation (EPR) test. The critical pitting potentials of as-sensitized as well as sensitized-laser melted specimens were determined by potentiodynamic anodic polarization method in a medium containing 0.5 M NaCl and 0.5 M H_2SO_4 at room temperature. Results indicated that upon laser melting the pitting resistance increased significantly. This increase was attributed to the elimination of the sensitized heterogeneous microstructure by laser melting. The microscopic examination of the pitted specimens showed only micropits that developed at the interfaces of oxide/sulfide inclusions of titanium and matrix.

Keywords austenitic stainless steels, laser surface melting, microstructural changes, pitting corrosion, sensitization

1. Introduction

Austenitic stainless steels (SS) form a major part of the structural materials for fast reactors because of their excellent mechanical properties at high temperatures and good corrosion resistance in general (Ref 1-3). However, during welding, heat treatment, and other fabrication procedures, these materials are often exposed to a temperature regime of 773 to 1073 K, which leads them to undergo a phenomenon known as sensitization. The deleterious effect of such a sensitizing heat treatment is the formation of chromium-rich carbides, namely, $M_{23}C_6$, along the grain boundaries and the subsequent creation of chromium-depleted narrow regions adjacent to such carbides (Ref 4-6). Such sensitized microstructures in stainless steels are highly prone to intergranular corrosion (IGC) and intergranular stress corrosion cracking (IGSCC). This problem requires the use of low-carbon containing SS and high-temperature solution annealing heat treatment. Incorporation of strong carbide forming alloying elements like titanium and niobium are advocated as remedial measures. It has been well-documented that the reduction in carbon content leads to lower mechanical strength; high-temperature solution annealing treatment would not be feasible for all components. The addition of nitrogen to the low-carbon containing austenitic stainless steel has been reported (Ref 7-11) to delay the onset of sensitization and to have better IGC and IGSCC resistance compared to conventional type 316L SS. However, prolonged thermal aging of the nitrogen-added austenitic stainless steel leads to sensitization.

U. Kamachi Mudali, M.G. Pujar, and **R.K. Dayal,** Metallurgy Division, Indira Gandhi Centre for Atomic Research, Kalpakkam-603 102, India.

In general, the sensitized microstructure is highly prone to pitting corrosion prior to IGC and IGSCC attack (Ref 12-14). The microstructural heterogeneities like chromium-rich carbides, chromium-depleted zones and their interfaces with the matrix present in the sensitized microstructure are the most susceptible sites for pitting attack. The presence of pits has been reported to give sites for stress corrosion and corrosion fatigue cracks to initiate and propagate leading to failure by fracture (Ref 15-17). To avert any equipment failure that could be caused due to the growth of pits and cracks, the sensitized microstructure has to be eliminated. Laser surface melting (LSM), a relatively new technique, is currently being used to modify the microstructure of the materials in a desired way by controlling the process parameters (Ref 18-22). Earlier works in this field show numerous applications wherein this technique has been successfully employed to reduce wear and corrosion. Recent works in the field of corrosion have shown the versatility of this technique in improving the IGC of sensitized type 316L SS (Ref 23-26). Importance of this technique is further highlighted by the in-situ use of this tool to modify the sensitized microstructure of the components, which are already sensitized in service (Ref 27). Kamachi Mudali and Dayal (Ref 25, 26) reported that such an improvement in IGC could be attributed to the dissolution of the chromium rich carbides or redistribution of such carbides into finer carbide particles and the elimination of the chromium depleted zones by the redistribution of the alloying elements during laser surface melting. Similar reasons imply that it is possible to improve the pitting corrosion resistance of sensitized austenitic SS components through laser surface melting by eliminating such probable pitting sites. Thus, while the bulk of the material is still sensitized, the surface can be modified through laser melting to eliminate the sensitized microstructure and make a surface material with improved IGC resistance.

Laser surface melting was employed to improve the pitting corrosion resistance of nitrogen-bearing type 316L SS sensitized at 923 K for various durations. This alloy was chosen as

the material of construction for the prototype fast breeder reactor (PFBR) to be built by the Department of Atomic Energy, India (Ref 1). Pulsed ruby laser was used for laser melting, and the resultant microstructures were examined by optical and scanning electron microscopy (SEM) attached with energy dispersive analysis of x-rays (EDAX). Potentiodynamic anodic polarization experiments were performed on the as-sensitized and sensitized-laser melted specimens in acidic, chloride containing medium to determine the pitting corrosion resistance. ASTM A 262 practice A test and electrochemical potentiokinetic reactivation (EPR) technique were employed to determine the degree of sensitization of the as-sensitized specimens. Morphological studies were performed after the above experiments by optical microscopy and SEM/EDAX.

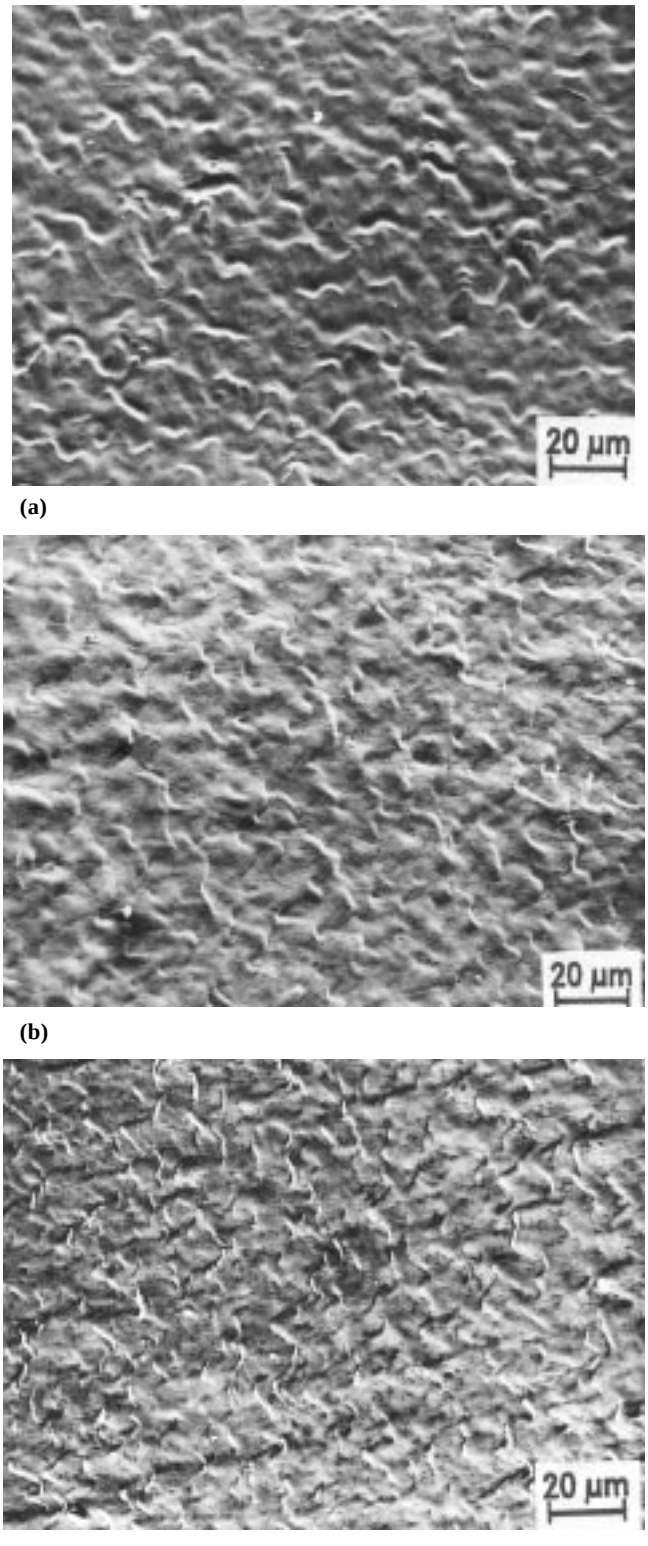

(a)

(b)

(c)

Fig.1 SEM micrographs of laser melted specimens at 6 J/pulse for (a) 2, (b) 3, and (c) 4 number of pulses

2. Experimental Work

2.1 Material and Heat Treatment

Nuclear grade nitrogen-bearing type 316L SS material was chosen; its chemical composition is given in Table 1. Initially, specimens of dimension 10 mm × 10 mm × 2 mm were prepared from a sheet and were given a solution annealing treatment at 1323 K for 30 min followed by quenching. Further, sensitizing heat treatment was given by thermally aging them at 923 K for 50, 200, 1000, and 2500 h durations. These specimens were polished up to 600 grit silicon carbide and were thoroughly cleaned with methanol prior to LSM.

2.2 Laser Surface Melting

Laser surface melting was carried out using a high power Q-switched pulsed ruby laser system (JK Industries, UK) with the following specifications: pulse width, 30 ns; wavelength, 693.4 nm; energy range, 1to10 J/pulse; and pulse frequency rate, 6 pulses/min. Laser irradiation was carried out at a calibrated energy of 2, 4, and 6 J/pulse with number of pulses ranging from 1, 2, 3, and 4. A pulse energy of 6 J/pulse with two successive pulses at the same spot was chosen as the optimum processing parameters, and all the specimen surfaces were melted using these parameters. The diameter of the melted region was approximately 6 mm. Complete melting of the surface was ensured by immediately observing the melted specimens visually and in a low power optical microscope. Further, the melted region of the specimens was observed in an optical microscope, and SEM was used to observe the surface topography.

Table 1 Chemical composition of type 316L SS

Element	Composition, wt%
Carbon	0.025
Nitrogen	0.0675
Sulphur	0.003
Phosphorus	0.025
Silicon	0.064
Manganese	1.68
Molybdenum	2.38
Nickel	10.12
Titanium	0.001
Niobium	0.045
Chromium	17.6
Iron	Bal

2.3 Evaluation of Degree of Sensitization

The aged specimens were electrolytically etched in a 10% ammonium persulfate solution at 6 V for 90 s as per ASTM A 262 practice A test (Ref 28). The resultant microstructure was classified as step, dual, and ditch structures. The EPR tests were carried out as per the procedures discussed by Clarke et al. (Ref 29): electrolyte is 0.5 M H_2SO_4 + 0.01 M NH_4SCN; scan rate is 6 V/h; passivation potential is +200 mV (saturated calomel electrode), and passivation time is 120 s; deaeration by argon purging. According to this test, a sensitized material shows significant reactivation peak current and charge density values that can be correlated to the degree of sensitization. The higher the reactivation peak current and charge density values, the higher is the susceptibility of the material to sensitization. After the electrolytic etching and EPR tests, the specimens were observed by optical microscope and SEM.

2.4 Pitting Corrosion Studies

Pitting corrosion studies were carried out by the potentiodynamic anodic polarization method in a solution containing 0.5 M NaCl and 0.5 M H_2SO_4 at room temperature. The electrode potential was measured with respect to a saturated calomel electrode (SCE). The electrolyte was continuously purged with argon gas to deaerate the solution, and the potential was anodically scanned at a rate of 10 mV/min from –500 mV (SCE) to a potential where a monotonic increase in the anodic current occurred. This potential above which stable pitting occurs was termed the critical pitting potential, E_{pp}. The details of the experimental procedures can be found in Ref 7, 30-35. After the tests, the specimens were observed in SEM/EDAX for the morphology of pits.

3. Results and Discussion

3.1 Surface Topography

Scanning electron microscopy observation of the LSM specimens showed that at lower pulse energies, 2 and 4 J/pulse, surface melting was incomplete whereas at 6 J/pulse melting was complete and uniform. The uniformity in the

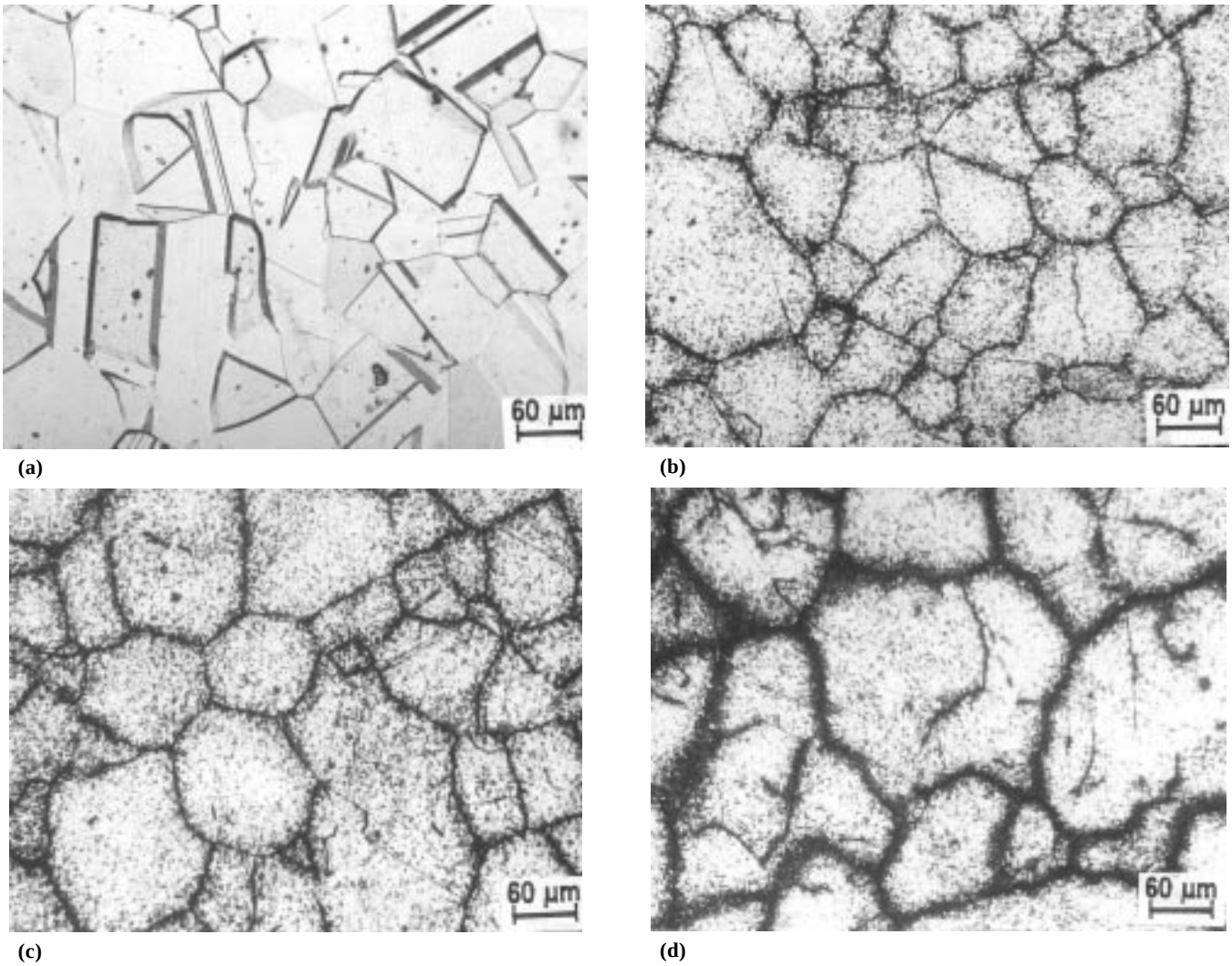

Fig. 2 Optical micrographs of type 316L SS sensitized at 923 K for (a) 50 h, (b) 200 h, (c) 1000 h, and (d) 2500 h after testing as per ASTM A 262 practice A test

surface topography is achieved by remelting the surface at the same spot by reirradiating at the same energy level. Hence, when remelting of the LSM surface was carried out at 6 J/pulse energy for 2, 3, and 4 pulses, it was clear (Fig. 1a-c) that at pulse repetition rates of 3 and 4, the surface topography became rough with the presence of numerous fine ridges. Such a surface could not be used for the pitting corrosion studies because the nonuniformities at the surface alone would act as pit nucleation sites. When the irradiation at 6 J/pulse with two successive pulses at the same spot is carried out, it is observed (Fig. 1c) that the surface is smooth and devoid of any roughness, which could be ideal for pitting corrosion studies. The surface and cross section of LSM specimens did not show any microcracks or micropores.

3.2 Degree of Sensitization

The results of electrolytic etching of all thermally aged specimens in 10% ammonium persulfate solution showed microstructures that are typically classified as step, dual, and ditch as per ASTM A 262 practice A specifications. Continuous grain boundary dissolution is termed ditch structure, which is normally observed in all the sensitized specimens. The microstructures observed are:

923 K/50 h → Step

923 K (200, 1000, and 2500 h) → Ditch

Table 2 Critical pitting potentials, E_{pp}, of as-sensitized and sensitized-laser melted specimens

	E_{pp}, mV	
Condition	**Before laser melting**	**After laser melting**
Solution annealed	940	...
Sensitized (923 K/50 h)	860	940
Sensitized (923 K/200 h)	610	740
Sensitized (923 K/1000 h)	340	640
Sensitized (923 K/2500 h)	510	620

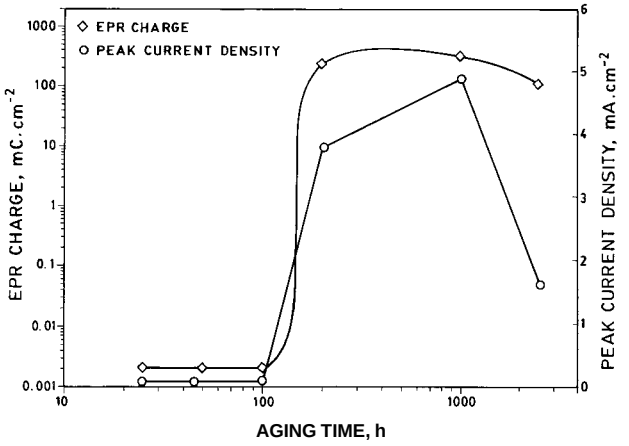

Fig. 3 EPR peak current density and charge density values of the sensitized type 316L SS as a function of aging time

Thus according to ASTM A 262 practice A, test specimens aged beyond 200 h at 923 K are likely to undergo sensitization. The typical microstructures obtained are shown in Fig. 2(a-d).

The EPR peak current density values obtained for all the aged specimens are given in Fig. 3, and it is very clear that as the aging time increased beyond 50 h, significant increase in the peak current density was noticed. However, a drop in the value was noticed at 2500 h, which could be due to the desensitization (i.e., redistribution of carbon and chromium to produce homogeneous carbon and chromium content throughout the structure) behavior of the alloy. A similar trend was noticed while calculating the EPR charge values (Fig. 3). Thus, in aging from 200 to 1000 h, significant carbide precipitation with chromium depleted zones are present, and at 2500 h, a desensitized microstructure with less chromium depleted zones are present. Such a microstructure would be first undergoing pitting attack prior to intergranular corrosion and intergranular stress corrosion cracking.

3.3 Pitting Corrosion Resistance

The potentiodynamic anodic polarization curves for the as-sensitized and sensitized and laser melted specimens are shown in Fig. 4 to 7. From these curves, the critical pitting

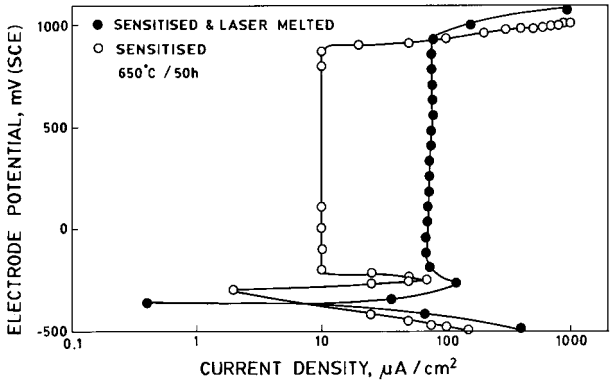

Fig. 4 Potentiodynamic anodic polarization curves of as-sensitized and sensitized-laser melted specimens (923 K/50 h) in acidic chloride medium

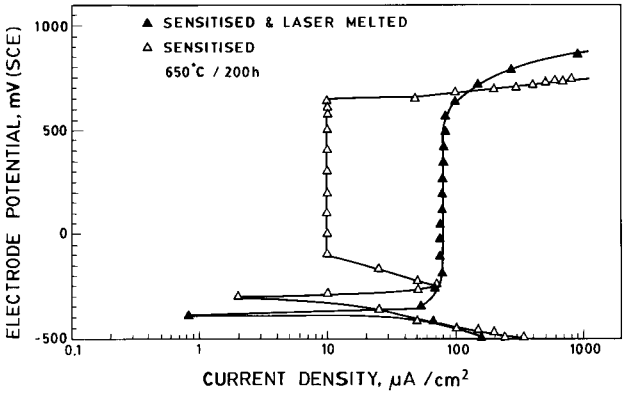

Fig. 5 Potentiodynamic anodic polarization curves of as-sensitized and sensitized-laser melted specimens (923 K/200 h) in acidic chloride medium

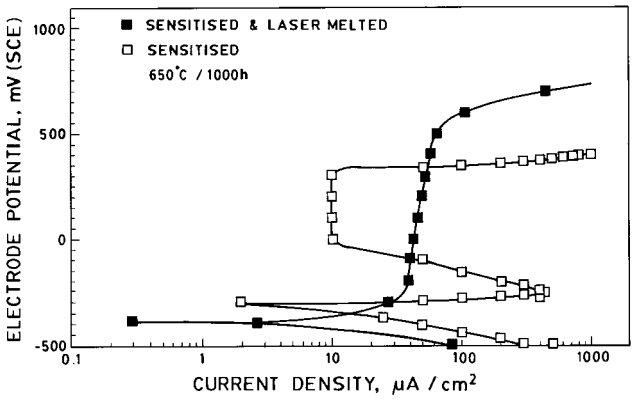

Fig. 6 Potentiodynamic anodic polarization curves of as-sensitized and sensitized-laser melted specimens (923 K/1000 h) in acidic chloride medium

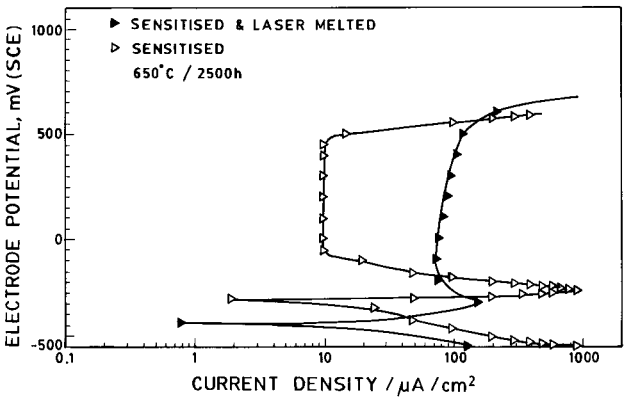

Fig. 7 Potentiodynamic anodic polarization curves of as-sensitized and sensitized-laser melted specimens (923 K/2500 h) in acidic chloride medium

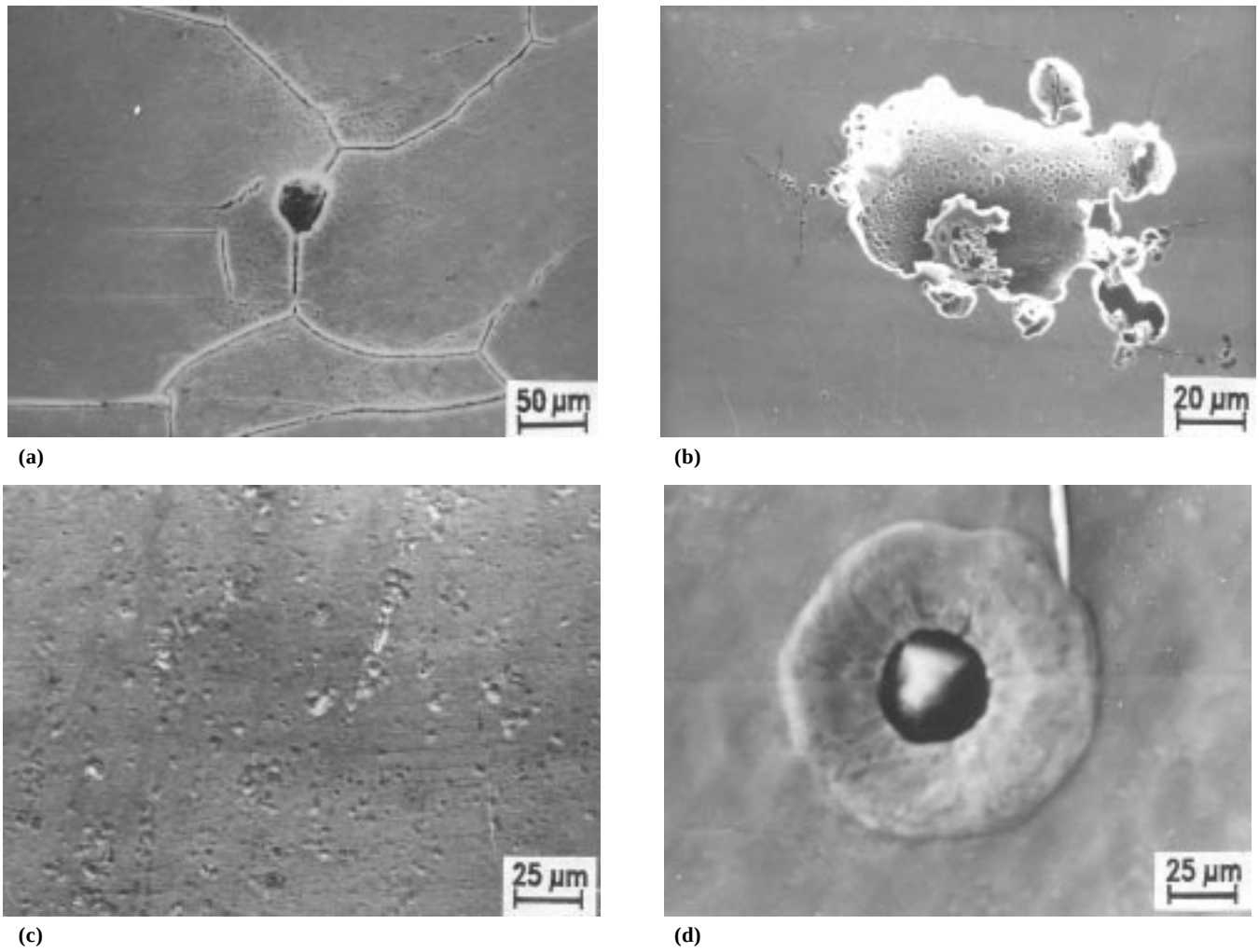

Fig. 8 SEM micrographs of pitted specimens of (a) and (b) sensitized condition, and (c) and (d) sensitized-laser melted condition

potentials were obtained for the specimens as shown in Table 2. It is clear that laser melting of the sensitized surface resulted in increased resistance to pitting as indicated by the increased values of the critical pitting potentials. Since the specimen aged for 50 h showed step structure indicating partially grown carbide precipitates and the formation of insignificant chromium depleted zones adjacent to them, the decrease in the E_{pp} value was not very significant after sensitization treatment.

Even then, the laser melting of the surface of this specimen resulted in a higher pitting potential compared to the as-sensitized specimen. Incidentally, this pitting potential was equal to that of solution annealed specimen without any sensitizing heat treatment. This indicated the superior pitting resistance of the sensitized specimen upon laser surface melting. The critical current density in the active region for the specimens aged for 1000 and 2500 h decreased significantly upon laser surface melting, and correspondingly a significant increase in the critical pitting potentials was noticed. In all cases, the laser melting resulted in a higher passivation current density for the specimens. This could be due to the rougher surface of the laser melted regions compared to the unmelted as-sensitized specimens and the quenching/thermal stresses introduced at the melted region due to rapid heating/quenching/resolidification reactions occurring at the surface during LSM (Ref 25). It is well known (Ref 36-38) that the presence of such stresses in the surface would reduce the pitting resistance by creating a weak and stressed passive film, which is more prone to damage by aggressive anions like chloride ions.

Laser surface melting could have resulted in dissolution or spheroidization of inclusions like MnS and FeS, and homogenization of chromium depleted regions and carbide/matrix interfaces and other probable pitting sites (Ref 19, 39-42). Also, laser melting has been reported (Ref 18, 21) to produce a near-amorphous structure that is microcrystalline in nature. However, once carbide precipitation is significant, laser melting could dissolve or redistribute such carbides into finer precipitates, as well as homogenize the chromium depleted zones by uniformly distributing the alloying elements, particularly chromium. It has been reported (Ref 19, 39-42) that the laser surface melting improved the pitting resistance by eliminating probable pitting sites like grain boundary precipitates, second phase precipitates, inclusions, and segregated interfaces. The dissolution of such sites and the uniform distribution of alloying elements would facilitate the formation of a stable passive film with improved pitting resistance. Tsuru and Latanision (Ref 42) also reported that the distribution of carbides and other precipitates uniformally in smaller sizes improved the pitting resistance. Thus sensitized-laser melted specimens showed a higher E_{pp} value compared to those of as-sensitized specimens. However, laser melting could have resulted in higher and similar improvements in pitting corrosion resistance for all sensitized specimens. The differences in the critical pitting potential values obtained for the laser melted specimens could be attributed to the density and distribution of carbide precipitates developed in the matrix after the sensitization treatment and the inclusions present. As the aging period increased, the density and growth of carbides increased leading to severe heterogeneity at the surface with complete network of wider chromium depleted zones (Ref 43). The energy of laser and the depth of laser melting obtained are not sufficient enough to create a completely homogeneous microstructure at the surface.

In as-sensitized specimens showed pitting attack at triple points and grain boundaries (Fig. 8a and b) because the microstructure containing $M_{23}C_6$ carbides and chromium depleted zones provided the pit nucleation sites. The pit morphological studies of the LSM specimens showed altogether different

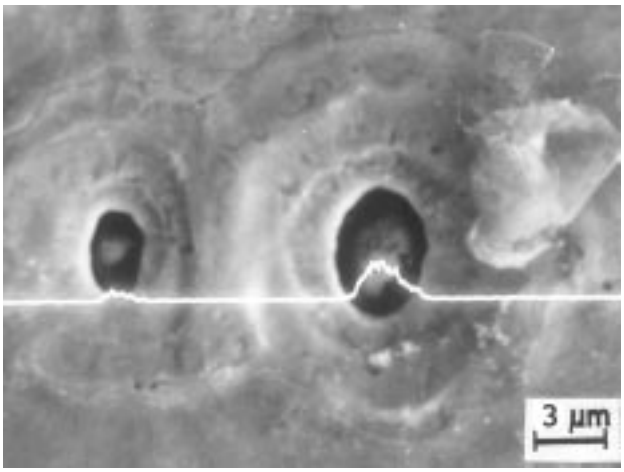

Fig. 9 SEM/EDAX observation showing the pitting attack at titanium-base inclusion/matrix interfaces

microstructural features. In all the microstructural observations carried under SEM, total absence of grain boundaries was prominently noted. Such a microstructure could positively improve pitting resistance because of the elimination of probable pit nucleation sites. Figures 8(c) and (d) show the SEM micrographs of the pitted specimens from the potentiodynamic anodic polarization study. Shallow micropits in the melted region of the sensitized-laser melted specimens were noticed. These micropits showed a different type of pit morphology, which cannot be correlated to the presence of chromiumdepleted zones or to the $M_{23}C_6$ carbides/matrix interfaces. An EDAX analysis of the melted zone was carried out to study the origin of such micropits. The EDAX analysis showed the presence of oxide and/or sulfide inclusions of titanium in the matrix (Fig. 9). Nevertheless, the melted specimens showed superior pitting resistance compared to the sensitized specimens.

4. Conclusions

Pitting corrosion studies were carried out on as-sensitized and sensitized-laser melted specimens of nitrogen-bearing type 316L SS. The following conclusions were drawn:

- The results of the ASTM A 262 practice A and the EPR tests on the specimens aged at 923 K for 50, 200, 1000, and 2500 h indicated an increased degree of sensitization from 50 to 1000 h, which decreased at 2500 h due to desensitization.
- Laser melting of the specimens at 6 J/pulse and for two successive pulses by pulsed laser resulted in uniform, defect free laser melted regions.
- Pitting corrosion studies on the sensitized-laser melted specimens showed significant improvement in E_{pp} values in comparison with the as-sensitized specimens. The critical current density significantly decreased for the sensitized-laser melted specimens aged at 1000 and 2500 h, whereas the critical passivation current density increased compared to as-sensitized specimens.

- The as-sensitized specimen pits nucleated at the chromium depleted regions and at the carbide/matrix interfaces. After laser melting only shallow micropits were found in the melted region, which were predominantly at inclusion/matrix interfaces.

Acknowledgments

The authors thank Dr. P. Rodriguez, Director, and Dr. Baldev Raj, Director, Metallurgy and Materials Group, and Dr. V.S. Raghunathan, Head, Metallurgy Division of IGCAR, Kalpakkam, for their keen interest in the work. Thanks are also extended to Mrs. R. Radhika of IGCAR for SEM observation of the specimens.

References

1. P. Rodriguez and S. L.Mannan, *Indian J.Technol.*, Vol. 28, 1990, p 281-295
2. J.T. Adrian Roberts, *Structural Materials in Nuclear Power Systems*, Plenum Press, 1981
3. J.B. Gnanamoorthy, *Proc. Indian Acad. Sci., Chem. Sci.,* Vol 97,1986, p 495-511
4. R.L. Cowan, II and C.S. Tedmon, Jr., *Advances in Corrosion Science and Technology,* Vol 3, M.G. Fontana and R.W. Staehle, Ed., Plenum Press, 1973, p 293-400
5. V. Cihal, *Intergranular Corrosion of Steels and Alloys,* Elsevier Publishing, 1984
6. S.M. Brummer, L.A. Charlot, and D.G. Atteridge, "Evaluation of Welded and Repair-Welded Stainless Steel for Light Water Reactor (LWR) Service," Reports NUREG/CR 3918, PNL-5186, Pacific Northwest Laboratories, 1984
7. U. Kamachi Mudali, *Studies on Pitting, Interganular Corrosion and Passive Film in Nitrogen-Bearing Austenitic Stainless Steels,* Ph.D. thesis, University of Madras, March 1993
8. J.J. Eckenrod and C.W. Kowach, in *Properties of Austenitic Stainless Steels and Their Weld Metals Influence of Slight Chemistry Variations,* ASTM STP 679, ASTM, 1979, p 17-41
9. C.L. Briant, R.A. Mulford, and E.L. Hall, *Corrosion,* Vol 38, 1982, p 468
10. T.A. Mozhi, K. Nishimoto, B.E. Wilde, and W.A.T. Clark, *Corrosion,* Vol 42, 1986, p 197
11. U. Kamachi Mudali, R.K. Dayal, J.B. Gnanamoorthy, and P. Rodriguez, *Metall. Trans. A,* Vol 27A, 1998, p 2881-2887
12. M.A. Streicher, *J. Electrochemical Society,* Vol 103, 1956, p 375
13. K. Osozawa, K. Bohnenkamp, and H.J. Engell, *Corrosion Sci.,* Vol 6, 1956, p 421
14. U. Kamachi Mudali, R.K. Dayal, J.B. Gnanamoorthy, and P. Rodriguez, *Iron and Steel Institute of Japan Int.,* Vol 36, 1996, p 799-806
15. Y. Kondo, *Corrosion,* Vol 45, 1989, p 7-11
16. J. Congleton and T.P. Wilks, *Fatigue Fracture Eng. Mater. Struc.,* Vol 11, 1988, p 139-148
17. M.O. Speidel, *Corrosion in Power Generating Equipment,* M.O. Speidel and A. Atrens, Ed., Plenum Press, 1984, p 85
18. C.W. Draper and J.M. Poate, *Int. Met. Rev.,* Vol 30, 1985, p 85-108
19. E.I. Meletis and R.F. Hochman, *JOM,* Vol 39, 1987, p 25-27
20. K. Mukherjee and J. Mazumder, *Lasers in Metallurgy,* Metallurgical Society of AIME, 1981
21. *Lasers in Materials Processing: Materials Processing-Theory and Practice,* M. Bass, Ed., Vol 3, North Holland Publishing, 1983
22. U. Kamachi Mudali, R.K. Dayal, J.B. Gnanamoorthy, S.M. Kanetkar, and S.B. Ogale, *Mater. Trans. JIM,* Vol 33, 1991, p 845-853
23. T.R. Anthony and H.E. Cline, *J. Appl. Phys.,* Vol 49, 1978, p 1248
24. J. de Damborena, A.J. Vazquez, J.A. Gonzalez, and D.R.F. West, *Surf. Eng.,* Vol 5, 1989, p 235
25. U. Kamachi Mudali and R.K. Dayal, *J. Mater. Eng. Perform.,* Vol 1, 1992, p 341-346
26. U. Kamachi Mudali, R.K. Dayal, and G.L. Goswami, *Surf. Eng.,* Vol 11, 1995, p 331-335
27. J. Stewart, D.B. Wells, P.M. Scott, and A.S. Bransdent, *Corrosion,* Vol 46, 1990, p 618-620
28. "Standard Recommended Practices for Detecting Susceptibility to Interganular Attack in Stainless Steels," ASTM A 262 Practice A, Vol 03.02, ASTM, 1986, p 2
29. W.L. Clarke, R.L. Cowan, and W.L. Walker, *Intergranular Corrosion of Stainless Alloys,* ASTM STP 656, ASTM, 1978, p 99
30. U. Kamachi Mudali, R.K. Dayal, T.P.S. Gill, and J.B. Gnanamoorthy, *Werkst. Korros.,* Vol 37, 1986, p 637-643
31. T.P.S. Gill, U. Kamachi Mudali, V. Seetharaman, and J.B. Gnanamoorthy, *Corrosion,* Vol 44, 1988, p 511-516
32. U. Kamachi Mudali, R.K. Dayal, T.P.S. Gill, and J.B. Gnanamoorthy, *Corrosion,* Vol 46, 1990, p 454-460
33. U. Kamachi Mudali, A.K. Bhaduri, and J.B. Gnanamoorthy, *Mater. Sci. Technol.,* Vol 42, 1990, p 475-481
34. U. Kamachi Mudali, H.S. Khatak, R.K. Dayal, and J.B. Gnanamoorthy, *J. Mater. Eng. Perform.,* Vol 2, 1993, p 135-140
35. U. Kamachi Mudali, R.K. Dayal, J.B. Gnanamoorthy, and P. Rodriguez, *Mater. Trans. JIM,* Vol 37, 1996, p 1568-1573
36. P.T. Cottrell, R.P. Frankenthal, G.W. Kammlott, D.J. Siconolfi, and C.W.J. Draper, *J. Electrochemical Society,* Vol 130, 1983, p 998-1001
37. G.T. Burstein and P.C. Pistorius, *Corrosion,* Vol 51, 1995 p 380-385
38. T. Chande, A. Ghose, and J. Mazumber, *Surf. Eng.,* Vol 3, 1987, p 53-58
39. E. McCafferty, P.G. Moore, J.D. Ayers, and G.K. Hubler, *Corrosion of Metals Processed by Directed Energy Beams,* C.R. Clayton and C.M. Preece, Ed., The Metallurgical Society of AIME, 1982, p 1-8
40. J.B. Lumsden, D.S. Gnanamuthu, and R.J. Moores, *Proc. Int. Symposium on Fundamental Aspects of Corrosion Protection by Surface Modification,* E. McCafferty, C.R. Clayton, and J. Oudar, Ed., The Electrochemical Society, 1984, p 122-129
41. J.B. Lumsden, D.S. Gnanamuthu, and R.J. Moores, *Proc. Int. Symposium on Fundamental Aspects of Corrosion Protection by Surface Modification,* E. McCafferty, C.R. Clayton, and J. Oudar, Ed., The Electrochemical Society, 1984, p 122-129
42. T. Tsuru and R.M. Latanision, *Corrosion and Corrosion Protection,* R.P. Frankenthal and F. Mansfield, Ed., The Electrochemical Society, 1981, p 238
43. S.K. Mannan, R.K. Dayal, M. Vijayalakshmi, and N. Parvathavarthini, *J. Nuclear Mater.,* Vol 126, 1984, p 1